Ultraslow diffusion in an exactly solvable non-Markovian random walk

M. A. A. da Silva,[1] G. M. Viswanathan,[2] and J. C. Cressoni[1]
[1]*Departamento de Física e Química, FCFRP, Universidade de São Paulo, 14040-903 Ribeirão Preto, SP, Brazil*
[2]*Departamento de Física Teórica e Experimental, Universidade Federal do Rio Grande do Norte, Natal, RN, 59078-900, Brazil*
(Received 21 November 2013; published 8 May 2014)

We study a one-dimensional discrete-time non-Markovian random walk with strong memory correlations subjected to pauses. Unlike the Scher-Montroll continuous-time random walk, which can be made Markovian by defining an operational time equal to the random-walk step number, the model we study keeps a record of the entire history of the walk. This new model is closely related to the one proposed recently by Kumar, Harbola, and Lindenberg [Phys. Rev. E **82**, 021101 (2010)], with the difference that in our model the stochastic dynamics does not stop even in the extreme limit of subdiffusion. Surprisingly, this small difference leads to large consequences. The main results we report here are exact results showing ultraslow diffusion and a stationary diffusion regime (i.e., localization). Specifically, the equations of motion are solved analytically for the first two moments, allowing the determination of the Hurst exponent. Several anomalous diffusion regimes are apparent, ranging from superdiffusion to subdiffusion, as well as ultraslow and stationary regimes. We present the complete phase diffusion diagram, along with a study of the persistence and the statistics in the regions of interest.

DOI: 10.1103/PhysRevE.89.052110 PACS number(s): 05.70.Ln, 05.40.−a, 02.50.−r, 87.23.Kg

I. INTRODUCTION

Perhaps the most important quantity determining the type of diffusion of a random walker is the asymptotic scaling of the mean square displacement (MSD) with time. The MSD is defined by $\langle \Delta x^2 \rangle = \langle (x - \langle x \rangle)^2 \rangle \sim t^{2H}$, and the asymptotic scaling exponent H is known as the Hurst exponent [1]. The linear dependence on time, with $H = 1/2$, is associated with the so-called normal diffusion. When the MSD changes at a faster or slower rate than "normal," the diffusion is termed anomalous. Anomalous diffusion [2–7] is categorized as subdiffusive for $0 < H < 1/2$, superdiffusive for $1/2 < H < 1$, or ballistic (or wavelike) for $H = 1$. Even faster superballistic diffusion with $\langle \Delta x^2 \rangle \sim t^3$ has been observed [8] in the study of turbulence in the atmosphere as early as 1926. Many systems have been shown to exhibit anomalous diffusion in areas as diverse as physics, chemistry, geophysics, biology, and economy [9–29]. More recently, anomalous diffusion has been observed in many experiments, such as self-motile active colloids [30], platinum deposition by plasma sputtering on a porous carbon substrate [31], ferrimagnetic maghemite nanoparticles [32], binary mixtures of hard particles confined to narrow pores [33], and many others [34]. Subdiffusive behavior has been reported, e.g., in semiconductors, polymers, and porous systems (see references in Ref. [5]). In microbiology, subdiffusion is widely observed as a method for transporting material inside living cells [35] (more references in Ref. [36]), possibly explained by the crowded environment within the cell [37]. Several tools have been used to describe anomalous dynamics, such as generalized diffusion equations [46], continuous time random walks [2,4,19,21,47–50], generalized master equations [51], generalized Langevin equation (GLE) [38,41–45], generalized thermodynamics [52,53], and fractional dynamical equations [5,12,54–56] (the latter considered as particularly suitable for describing subdiffusion and slow relaxation processes).

With the use of the mathematical tools above, other patterns of anomalous diffusion processes have been uncovered, such as the logarithmic corrections to scaling, of the type $\langle x^2(t) \rangle \sim t \log t$ (marginally superdiffusive) and $\langle x^2(t) \rangle \sim t/\log t$ (marginally subdiffusive) obtained using GLE [38] and CTRW [39,40], respectively. These models display transitions from one diffusion type to another by suitable changes to the model's parameter. Another type of diffusive behavior is ultraslow diffusion, also called strong anomalous diffusion or superslow diffusion. In this case, the MSD grows logarithmically with time, i.e., $\langle x^2(t) \rangle \sim \log^{\nu} t$ with $\nu > 0$ as found in Sinai's model [57] (see Refs. [12,58–60] and references therein). Theoretical models generating USD are rare [61], especially in discrete-time random walks, which require some sort of explicit microscopic mechanism. On the experimental side, it has recently been suggested that individual movement patterns of humans and capuchin monkeys may exhibit ultraslow diffusion [62].

Another approach to study diffusion processes is the well-known discrete time random walk. Random walks are very convenient for microscopic modeling. They allow a direct description of the physics underlying the stochastic dynamics and have been broadly used to describe stochastic processes in statistical physics [63]. More recently, Schütz and Trimper [64] introduced an exactly solvable discrete-time non-Markovian random walk model that retains the full memory history of previous decisions, leading to a memory-driven superdiffusive behavior separated from the normal diffusion phase by a marginally superdiffusive regime of the type $\langle x^2(t) \rangle \sim t \log t$. The model became known as the elephant random-walk (ERW) model, as an allusion to the fact that "elephants always remember," an expression used by the authors of the original paper. A continuous time generalization of the ERW was conducted by Paraan and Esguerra [65], along with a discussion on the non-Gaussian behavior associated with the superdiffusive regime. The ERW model was later generalized to include damage to the memory [66], which uncovered

another superdiffusive regime endowed with log-periodic oscillations within a parameter region driven by negative feedback. The dynamics proposed by Schütz and Trimper was generalized by Kumar, Harbola, and Lindenberg [67] (KHL) which included pause probabilities in the dynamics, leading to the emergence of subdiffusion.

In this paper we propose a random-walk model that follows closely the dynamics of the non-Markovian ERW model, thereby including the long-range time memory correlations. The ERW memory model defines a simple non-Markovian stochastic dynamics with a clear microscopic origin. It has been shown that it provides a solid microscopic foundation for a Fokker-Planck equation with a time-dependent term (see, for example, Refs. [64,76]). The unbounded long-time memory is essential to confer the non-Markovian character to the dynamics leading to anomalous (super) diffusion. However, we also include pause probabilities, in some extent inspired in the KHL model. The pauses are included focusing on: (a) leaving the ERW dynamics intact and (b) allowing the pausing controlling parameter to assume a wide range of values, leading to new diffusion regimes. This general model can be shown to contain the KHL model as a particular case. The pauses act like traps that slow down the particle's speed allowing for other diffusion types to appear, as can be seen in the KHL model. Notice that the original dynamics of the ERW model contains no pauses, but a damping-like term is inherently included in the Fokker-Planck equation (FPE) of the model. This can be easily seen by comparing the FPE in Ref. [64] with Eq. (5) in Ref. [68]. We choose to introduce pause probabilities as a way to trap down the random particle, thereby enhancing the damping effect and ultimately leading to subdiffusion and strong anomalous diffusion (such as ultraslow and stationary diffusions). The functional form for the pausing probability is chosen in such a way that the solution becomes analytically treatable. The inclusion of pauses (or traps) causes the emergence of new diffusion regimes, e.g., with $H < 1/2$. Based on an heuristic approach, we write the functional form for the probability to pause, namely $P_s(t)$, as a power law of time. This special formulation of the model yields exact solutions for the first two moments with the outcome of several diffusion regimes, such as: superdiffusive, subdiffusive, ultraslow, and stationary regimes. The stationary regimes correspond to $H < 0$ and are thus related to unusually strong antipersistent correlations, in contrast to the other types of persistence, usually classified according the Hurst exponent, i.e., $0 < H < 1/2$ and $1/2 < H < 1$, correspond to negative (antipersistent) correlations and positive (persistent) correlations, respectively, while $H = 1/2$ is relative to an uncorrelated Brownian process. Negative values for the Hurst exponents are abundant in the study of diffusive systems, particularly in biophysics, geophysics, and materials science [69–74]. The model's regimes are obtained simply by suitably tuning the model's parameters. To the best of our knowledge, this is the first discrete-time random-walk model to display such a rich variety of diffusion regimes.

The paper is organized as follows. Section II describes the model's dynamics and Sec. III discusses the equations of motion. The first and second moments are derived in Secs. IV and V, respectively. Section VI discusses the results, and in Sec. VII the conclusions are drawn.

II. THE MODEL

We describe a discrete-time random-walk model in one dimension with unitary time steps and long-range memory correlations. The model generalizes the elephant random-walk model of Schütz and Trimper [64], by introducing an explicit time-dependent random decision to induce pauses in the walk. More specifically, consider the general position of the walker at time t, represented by X_t. At time $t+1$, the walker moves to a neighboring site, $X_{t+1} = X_t + \sigma_{t+1}$, where the stochastic variable σ takes on the values $\sigma_{t+1} = \pm 1,0$, with $\sigma_{t+1} = +1$ ($\sigma_{t+1} = -1$) for a right (left) step and $\sigma_{t+1} = 0$ for a pause. The choice of a particular value of σ_{t+1} starts with a random decision obtained from a probabilistic equation, namely $P_w(t) + P_s(t) = 1$. In this equation, $P_s(t)$ represents the probability to pause the motion, whereas $P_w(t)$ stands for the probability to walk. Therefore, we set $\sigma_{t+1} = 0$ with probability $P_s(t)$ and $\sigma_{t+1} = \pm 1$ with probability $P_w(t)$. The functional form of $P_s(t)$ is discussed below. Except for the pauses, the dynamics in our model is the same used for the elephant random-walk model [64]. This means that, when $\sigma_{t+1} \neq 0$, we choose a previous time t' from a uniform distribution, such that $1 \leqslant t' \leqslant t$ and $\sigma_{t'} \neq 0$, and set σ_{t+1} according to

$$\sigma_{t+1} = \begin{cases} + & \sigma_{t'} \quad \text{with probability} \quad p \\ - & \sigma_{t'} \quad \text{with probability} \quad q \end{cases} . \tag{1}$$

Although $p + q = 1$, we shall keep both parameters, for clarity, until the end of the calculations. Equation (1) means that the decision at t' is accepted with probability p or rejected with probability q. All the previous history of the walker prior to $t+1$ is used in the decision process, which confers a non-Markovian character to the model. The initial conditions are set in such a way that $X_0 = 0$, and at $t = 0$ the walker moves one step to the right or left with probability s or $1 - s$, respectively, thereby setting $X_1 = \pm 1$. It is essential that the walker effectively moves at the initial time, so that the ERW rules can be applied.

The first model to introduce pause probabilities within the dynamics of the ERW model was proposed by Kumar *et al.* [67], leading to subdiffusion. Here we follow a different approach, by defining the pause probabilities in a way that, besides preserving the original ERW dynamics, leads to the emergence of new diffusion regimes. This approach induces, for example, the outcome of regimes slower than subdiffusion, as shown below. We follow a heuristic reasoning to derive a functional form for $P_s(t)$. The pauses act like traps, slowing down the particle and reducing its speed $v(t)$. Thus, classically, we can write $dv/dt = -\mu v$ with $\mu(t) = \lambda/t$ ($\lambda > 0$). This leads to a velocity that decays with time as a power law, i.e., $v(t) \sim t^{-\lambda}$. In order to comply with this form for $v(t)$ the pause probability must follow a power-law dependence with time. It can be written as $P_s(t) = 1 - At^{-\lambda}$ ($t > 0$, $\lambda \geqslant 0$). For simplicity we assume that $P_s(t)$ is position independent. We also take only positive values for the coefficient A, which causes the pause probability to increase with time for $\lambda > 1$. The occurrence of pauses can then be fine tuned by suitable choices of λ, with immediate effects on the diffusion behavior. Notice that a time-independent form for $P_s(t)$ would not have

any effect on the asymptotic diffusive behavior of the walker. In fact, this would only lead to a linear rescaling of the time parameter, namely $t \to at$. A linear rescaling cannot modify the asymptotic behavior of the model, which is related to the exponent of t.

In the next sections we study this model and its consequences to the diffusive regimes of the walker.

III. THE EQUATIONS OF MOTION

We now derive analytical expressions for the first two moments of the model. In what follows we shall work with $\alpha = p - q =$, or $\alpha = 2p - 1$ (since $p + q = 1$). It turns out that the results can be readily parametrized in terms of α, although the physical meanings of p and q are more evident.

Let $n_f(t)$ and $n_b(t)$ denote the number of steps taken in the forward and backward directions at time t, respectively. If $n_t = n_t(t)$ represents the total number of steps taken at time t, then the probability that a right step has been taken up to time t is given by $n_f(t)/n_t$. Similarly, $n_b(t)/n_t$ is the probability that the walker took a left step up to time t. The effective probabilities $P^+_{\rm eff}(t)$ and $P^-_{\rm eff}(t)$ of taking a step forward and backward at time $t+1$ ($t \geqslant 1$) are then given by

$$P^+_{\rm eff}(t) = \frac{n_f(t)}{n_t} p + \frac{n_b(t)}{n_t} q$$

and

$$P^-_{\rm eff}(t) = \frac{n_b(t)}{n_t} p + \frac{n_f(t)}{n_t} q,$$

respectively. Notice that $P^+_{\rm eff}(t)$ and $P^-_{\rm eff}(t)$ are conditional probabilities, since they represent the probability of taking right or left steps at $t+1$, given the history of the process embodied in the knowledge of the number of right and left steps up to time t. We now define the probabilities for right and left steps as $P^f_w \equiv P^f_w(t) = P^+_{\rm eff}(t) P_w(t)$ and $P^b_w \equiv P^b_w(t) = P^-_{\rm eff}(t) P_w(t)$, with $P^f_w + P^b_w = P_w(t)$, and write the effective value of $\sigma^{\rm eff}_{t+1}$ as $\sigma^{\rm eff}_{t+1} \equiv P^f_w - P^b_w$. In terms of the conditional probabilities $P^+_{\rm eff}(t)$ and $P^-_{\rm eff}(t)$, we can write

$$\begin{aligned}\sigma^{\rm eff}_{t+1} &= [P^+_{\rm eff}(t) - P^-_{\rm eff}(t)] P_w \\ &= \left[\frac{n_f(t)}{n_t}(p-q) - \frac{n_b(t)}{n_t}(p-q)\right](1 - P_s),\end{aligned}$$

where $P_w \equiv P_w(t)$ and $P_s \equiv P_s(t)$. In terms of $\alpha = p - q$ we can write $\sigma^{\rm eff}_{t+1} = (\alpha/n_t)(n_f - n_b)(1 - P_s)$, which gives $\sigma^{\rm eff}_{t+1} = (\alpha/n_t) X_t (1 - P_s)$. In this equation $X_t = n_f(t) - n_b(t)$ is the position of the walker at time t. However, if we denote the total number of pauses at time t by $n_s \equiv n_s(t)$, we can write $n_t = n_f(t) + n_b(t)$ and $n_t + n_s = t$, which gives $n_t = t - n_s$. Then

$$\sigma^{\rm eff}_{t+1} = \frac{\alpha}{t - n_s} X_t (1 - P_s), \tag{2}$$

where $n_s(t) = \int_{t_0}^{t} P_s(t) dt$. In this equation, t_0 represents a temporal cutoff scale which reflects the breakdown of the continuum approximation for $t \to t_0$. For the initial condition, we then set $x(t = t_0) = x_0$. We now use the power-law functional form for the pause probability, introduced in the previous section, namely,

$$P_s(t) = 1 - A t^{-\lambda} \quad (\lambda \geqslant 0) \tag{3}$$

where $0 < A \leqslant t_0^{\lambda}$, since $0 \leqslant P(t_0) = 1 - A t_0^{-\lambda} \leqslant 1$, which allows the number of pauses $n_s(t)$ to be written as

$$n_s(t) = \int_{t_0}^{t} (1 - A t^{-\lambda}) dt. \tag{4}$$

The cases $\lambda \neq 1$ and $\lambda = 1$ must be treated separately for the determination of $\sigma^{\rm eff}_{t+1}$.

For $\lambda \neq 1$, we can write $n_s(t)$ as

$$n_s(t) = \left(t - A\frac{t^{1-\lambda}}{1-\lambda}\right) - \left(t_0 - A\frac{t_0^{1-\lambda}}{1-\lambda}\right) (\lambda \neq 1), \tag{5}$$

from which follows, by rearranging the terms, that $t - n_s = A_0 + A t^{1-\lambda}/(1-\lambda)$. Therefore, Eq. (2) can be written as

$$\sigma^{\rm eff}_{t+1} = \frac{\alpha A t^{-\lambda}}{A_0 + [A/(1-\lambda)] t^{1-\lambda}} X_t \quad (\lambda \neq 1). \tag{6}$$

For $\lambda = 1$ we have $P_s(t) = 1 - A/t$ and therefore Eq. (4) can be integrated for $t_0 \geqslant 1$ to give $t - n_s = t_0 + A \ln(t/t_0)$. We can now insert this back into Eq. (2), with $1 - P_s(t) = A/t$, and write

$$\sigma^{\rm eff}_{t+1} = \frac{\alpha A t^{-1}}{t_0 + A \ln(t/t_0)} X_t \quad (\lambda = 1). \tag{7}$$

The equations of motion for the model can now be written according to the parameter λ. From $X_{t+1} = X_t + \sigma_{t+1}$ we note that σ_{t+1} represents the step or "velocity" at time t. Thus, in the asymptotic limit of large t we can write $\langle \sigma^{\rm eff}_{t+1} \rangle = dx/dt$, and thus Eqs. (6) and (7) become

$$\frac{dx}{dt} = \frac{(1-\lambda)\alpha}{A t^{1-\lambda} + A_0(1-\lambda)} A t^{-\lambda} x \quad (\lambda \neq 1) \tag{8}$$

and

$$\frac{dx}{dt} = \frac{\alpha}{t_0 + A \ln(t/t_0)} A t^{-1} x \quad (\lambda = 1), \tag{9}$$

respectively. Equations (8) and (9) constitute the equations of motion of the model. They are the basic equations used in the derivation of the 1st and 2nd moments below.

The computation of the moments must be done separately according to $\lambda \neq 1$ or $\lambda = 1$. This is done in the next sections. A summary of the results is given in Table I.

IV. FIRST MOMENT CALCULATION

A. First moment for $\lambda \neq 1$

The first moment $x(t) \equiv \langle x(t) \rangle$ for $\lambda \neq 1$ is the solution of Eq. (8), given by

$$x(t) = C_1 \left(\frac{A}{1-\lambda} t^{1-\lambda} + A_0\right)^{\alpha} |1 - \lambda|^{\alpha} \quad (\lambda \neq 1).$$

With the initial condition $x(t = t_0) = x_0$ the constant C_1 obeys $x_0/C_1 = |1-\lambda|^{\alpha} [A/(1-\lambda) t_0^{1-\lambda} + A_0]^{\alpha}$. Thus, for $t \gg t_0$ we can write

$$x(t) \sim C_1 (1-\lambda) \left(\frac{A}{1-\lambda}\right)^{\alpha} t^{(1-\lambda)\alpha} \quad (\lambda < 1) \tag{10}$$

TABLE I. Summary of the results for the first $[x(t)]$ and second $[x_2(t)]$ moments, as a function of λ. The K_i are constants and $\alpha = p - q$. A logarithmic correction to power law is noted for $\lambda < 1$ when $\alpha = 1/2$. Ultraslow diffusion occurs for $\lambda = 1$ and $\alpha \neq 1/2$, and becomes even slower for $\alpha = 1/2$. Stationary diffusion with $H < 0$, is noted for $\lambda > 1$.

1st moment		
$\lambda < 1$		$x(t) \sim K_0 t^{(1-\lambda)\alpha}$
$\lambda = 1$		$x(t) = x_0[1 + (A/t_0)\ln(t/t_0)]^\alpha$
$\lambda > 1$		$x(t) \sim K_1 + K_2 t^{1-\lambda}$
2nd moment		
$\lambda < 1$	$(\alpha < 1/2)$	$x_2(t) \sim t^{1-\lambda}$
	$(\alpha = 1/2)$	$x_2(t) \sim t^{1-\lambda}\ln t$
	$(\alpha > 1/2)$	$x_2(t) \sim t^{2\alpha(1-\lambda)}$
$\lambda = 1$[a]	$(\alpha \neq 1/2)$	$x_2(t) \sim K_3 + K_4(\ln t)^2$
	$(\alpha = 1/2)$	$x_2(t) \sim K_5 + K_6(\ln t)[\ln(\ln t)]$
$\lambda > 1$[b]		$x_2(t) \sim K_7 + K_8 t^{1-\lambda}$

[a]Ultraslow diffusion for $\lambda = 1$.
[b]Stationary diffusion for $\lambda > 1$.

and

$$x(t) \sim C_1(\lambda - 1)A_0^\alpha\left(1 + \frac{\alpha A t^{1-\lambda}}{A_0(1-\lambda)}\right) \quad (\lambda > 1). \tag{11}$$

B. First moment for $\lambda = 1$

For $\lambda = 1$ we must integrate Eq. (9), i.e.,

$$\int \frac{dx}{x} = A\alpha \int \frac{dt}{t[t_0 + A\ln(t/t_0)]}$$

to give

$$\begin{aligned} \ln x &= \alpha \ln[t_0 + A\ln(t/t_0)] + C \\ &= \ln\{C_0[t_0 + A\ln(t/t_0)]^\alpha\} \end{aligned} \tag{12}$$

and then $x = C_0[t_0 + A\ln(t/t_0)]^\alpha$. Since $x_0 = C_0 t_0^\alpha$, we can write

$$x = x_0\left[1 + \frac{A}{t_0}\ln(t/t_0)\right]^\alpha \quad (\lambda = 1). \tag{13}$$

If we had chosen an exponential form for $P_s(t)$, the first moment would be an exponentially decaying function of time. The pause probability written as an increasing power law with time leads to power-law behavior for the first and second moments, as desired.

V. SECOND MOMENT CALCULATION

We now turn our attention to the second moment. We start with the basic equation $X_{t+1} = X_t + \sigma_{t+1}$, which gives

$$X_{t+1}^2 = X_t^2 + 2\sigma_{t+1}X_t + \sigma_{t+1}^2,$$

and thus

$$\langle X_{t+1}^2\rangle = \langle X_t^2\rangle + 2\langle\sigma_{t+1}X_t\rangle + \langle\sigma_{t+1}^2\rangle. \tag{14}$$

Note that $\langle\sigma_{t+1}^2\rangle = (+1)^2 P_w^f + (-1)^2 P_w^b + (0)^2 P_s$, where P_s is the probability to pause and P_w^f (P_w^b) is the probability for a right (left) step, as defined above. Thus, we can write $\langle\sigma_{t+1}^2\rangle = P_w^f + P_w^b = 1 - P_s = At^{-\lambda}$, and Eq. (14) now reads

$$\langle X_{t+1}^2\rangle = \langle X_t^2\rangle + 2\langle\sigma_{t+1}X_t\rangle + At^{-\lambda}. \tag{15}$$

This will be the basic equation, valid for any $\lambda \geqslant 0$, to be used in the evaluation of the second moment. In this expression we shall determine the average value of $\langle\sigma_{t+1}X_t\rangle$ using the effective value $\sigma_{t+1}^{\text{eff}}$ determined above (see also Ref. [75]); i.e.,

$$\langle\sigma_{t+1}X_t\rangle = \langle\sigma_{t+1}^{\text{eff}}X_t\rangle, \tag{16}$$

valid for any $\lambda \geqslant 0$.

A. Second moment for $\lambda \neq 1$

The calculation of the second moment for $\lambda \neq 1$ involves the use of Eqs. (15) and (16) along with Eq. (6) for $\sigma_{t+1}^{\text{eff}}$. The time derivative of the second moment can then be written as (see Appendix)

$$\frac{dx_2}{dt} = \frac{2\alpha A t^{-\lambda}}{A_0 + [A/(1-\lambda)]t^{1-\lambda}}x_2 + At^{-\lambda} \quad (\lambda \neq 1),$$

where $x_2(t) \equiv \langle X_2(t)\rangle$. Integration gives

$$x_2(t) \sim \begin{cases} \{A/[(1-\lambda)(1-2\alpha)]\}t^{1-\lambda} & (\alpha < 1/2) \\ [C_0A^{2\alpha}/(1-\lambda)^{2\alpha}]t^{2\alpha(1-\lambda)} & (\alpha > 1/2) \\ At^{1-\lambda}\ln t & (\alpha = 1/2) \end{cases}$$

for $\lambda < 1$ and $t \gg t_0$. For $\lambda > 1$ and $t \gg 0$, the result is given by

$$\begin{aligned} x_2(t) \sim{}& \frac{A_0}{2\alpha}\ln[A_0(\lambda-1)] + C_0A_0^{2\alpha} \\ & - \frac{A}{\lambda-1}\left\{1 + \ln[A_0(\lambda-1)] + 2\alpha C_0 A_0^{2\alpha-1}\right\}t^{1-\lambda} \end{aligned} \tag{17}$$

as seen from Eq. (A2). Notice that for $\lambda > 1$ the number of pauses is even greater than the maximum number of pauses allowed by the Kumar-Harbola-Lindenberg (KHL) model. In this case, the second moment remains finite, due to the additive constant in Eq. (17). This means that the width of the distribution does not grow with time, as opposed to what is observed in the ERW, even for $p = 1/2$ (traditional

RW). Likewise, the first moment also remains finite in the asymptotic limit, according to Eq. (11). Therefore, the particle remains confined in a finite-space region. This is one of the distinguished features of the model, not commonly observed in discrete-time RW models in the literature.

B. Second moment for $\lambda = 1$

For $\lambda = 1$ we use Eqs. (15) and (16), along with Eq. (7) for $\sigma_{t+1}^{\rm eff}$. A differential equation for $x_2(t)$ is obtained in the Appendix given by Eq. (A3), i.e.,

$$\frac{dx_2}{dt} = 2\frac{A\alpha(1-\lambda)}{t[t_0 + A\ln(t/t_0)]}x_2 + At^{-\lambda}. \tag{18}$$

When this equation is integrated it gets separated into two forms, according to the value of α. The solutions are derived in the Appendix. One gets

$$x_2(t) = C_1[t_0 + A\ln(t/t_0)]^2 + \frac{t_0 + A\ln(t/t_0)}{1-2\alpha},$$

for $\alpha \neq 1/2$, and

$$x_2(t) = [t_0 + A\ln(t/t_0)]\ln[t_0 + A\ln(t/t_0)] + C_2[t_0 + A\ln(t/t_0)],$$

for $\alpha = 1/2$. In this case, the second moment has a logarithmic correction to the power law. Expressions for the constants are derived in the Appendix.

VI. MODEL'S STATISTICS

We also briefly present some aspects of the statistics associated with the diffusion regimes of the model. Some results are already known for $\lambda = 0$, i.e., the ERW model: the propagator is Gaussian for $\alpha < 0$ and non-Gaussian for $\alpha > 1/2$ [64,76]; for $0 < \alpha < 1/2$ the propagator is seemingly Gaussian, but some doubts remain [76]. In Figs. 4 and 5 below we take into account the effect of the pause probabilities in the statistics. We also study the statistics when $\alpha > 1/2$ (or $p > 3/4$). The probability density functions (PDFs) for the persistence length and the walker's position are also determined. This is discussed below in Fig. 5 for $\lambda \geqslant 0$.

The diffusion regimes are also usually characterized as persistent ($H > 1/2$) and antipersistent ($0 < H < 1/2$), while for $H = 0$ the position series corresponds to the uncorrelated Gaussian white noise. Antipersistent regimes associated with $H < 1/2$, means that fluctuations tend to induce stability (via some sort of negative feedback mechanism). This is fine for $\alpha < 0$, or $p < q$, since in this region a negative feedback mechanism is naturally embodied in the dynamics of the ERW model. However, it is interesting to note the coexistence of antipersistent regimes (with $H < 1/2$) with escape regimes (those for which $\langle x(t)\rangle$ diverges). Moreover, the escape region occurs for $\alpha > 0$, meaning that $p > q$. This indicates that the underlying feedback (microscopic) is positive, which should induce persistence [as in the superdiffusive region (iv)] rather than antipersistence. We believe that the microscopic effects are diminished (or even totally destroyed) by memory effects. This happens for $\lambda = 0$ (or the ERW model) and $p = 0$, for example (notice that $H = 1/2$ in this case; see Fig. 1). More studies are necessary to clarify these points as in Refs. [77,78].

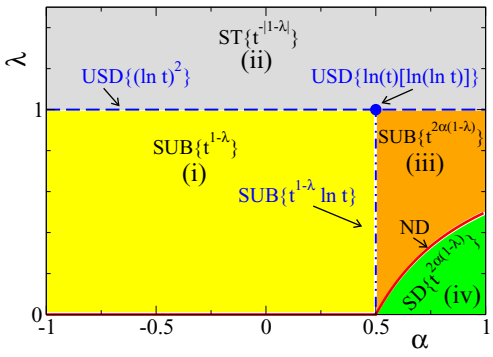

FIG. 1. (Color online) Diffusion regimes of the model showing the large time scaling behavior of the second moment. The notation SD, ND, SUB, USD, and ST stand for superdiffusive, normal diffusive, subdiffusive, ultraslow diffusion, and stationary diffusion, respectively. The logarithmic regimes are shown along the (blue) dashed ($\langle x^2\rangle \sim (\ln t)^2$) and dash-double-dotted ($\langle x^2\rangle \sim t^{1-\lambda}\ln t$) lines and also on the point $(\alpha,\lambda) = (1/2,1)$, for which $\langle x^2\rangle \sim (\ln t)[\ln(\ln t)]$. The diffusion is ultraslow (USD) for $\lambda = 1$. Normal diffusive regimes are restricted to the (red) continuous line. Region (iv) corresponds to the superdiffusive regime (SD). For $\lambda > 1$ the regime is stationary, with $\langle x^2\rangle$ becoming independent of time for large times. The main point to note are the USD and stationary regimes, which are absent in all previous models in the family of the elephant random walk (ERW).

VII. RESULTS AND ANALYSIS

Table I summarizes the analytical results for the first two moments for asymptotically large times. The Hurst exponent H can be derived from the asymptotic behavior of the second moment $x_2(t)$. This allows us to derive the diffusion regimes, as shown in Fig. 1. Regions (i) and (iii) indicate the subdiffusive regimes (SUB), and the superdiffusive regime (SD) is indicated in region (iv). For $\lambda > 1$ the Hurst exponent is negative, i.e., $H = -|1-\lambda|/2 < 0$. We are terming this regime as stationary (ST). Ultraslow diffusion exists on the (blue) dashed line ($\lambda = 1$). Normal diffusion is found on the (red) continuous line.

In Fig. 1, we can also determine the regions in the phase diagram for which there is escape in the asymptotic limit, i.e., when $\langle x(t)\rangle$ diverges for large times. According to Eqs. (10) and (13) we see that the escape regime exists when the conditions $\lambda < 1$ and $\alpha > 0$ are simultaneously met. Such an escape regime contains regions (iii), (iv), and the right part of region (i), for which $\alpha > 0$. There is no escape for all other combinations of the pair (α, λ).

Figure 2 shows the Hurst exponent $H = H(\lambda)$ as a function of λ for $\alpha = 0.9$. For this value of α (or $\alpha > 1/2$, in general) one crosses five regimes in the phase diagram with continuously decreasing persistence, as λ ranges from small values for the superdiffusive regime, through the intermediate values for the subdiffusive regime to larger values ($\lambda \geqslant 1$) for the ultraslow and stationary regimes. This figure illustrates the rich variety of regimes encompassed by the model that can be obtained by tuning one single parameter. The transition between different diffusion types is always smooth. This seems to be a general feature associated with these transitions. It can also be seen in other theoretical studies, like: (a) transition between subdiffusive and normal behavior crossing over an

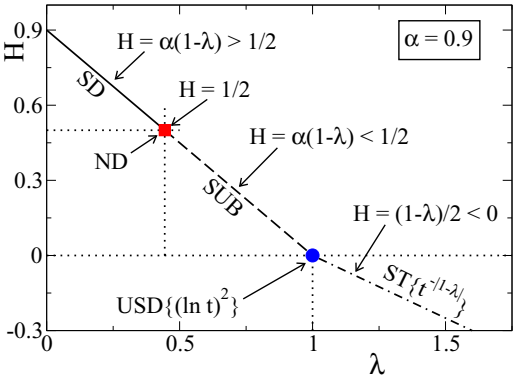

FIG. 2. (Color online) The variation of the Hurst exponent with λ for $\alpha = 0.9$ showing the continuous transition across all the phases: from the superdiffusive regime [$H = \alpha(1-\lambda) > 1/2$, continuous line] for small λ through the subdiffusive regime [$H = \alpha(1-\lambda) < 1/2$, dashed line] to the stationary phase [$H = (1-\lambda)/2 < 0$, dash-dotted line] for $\lambda > 1$. The notation for the diffusion regimes is the same as described in the legend of Fig. 1. Negative Hurst exponents are unusual and should be treated with extra care. Here, a negative Hurst exponent does not mean that the random-walk propagator becomes less wide at long times but rather that the width approaches a constant aysymptotically.

intermediate marginally subdiffusive logarithmic behavior in Refs. [39,40], and (b) between superdiffusion and subdiffusion and stationary diffusion separated by lines describing normal diffusion and logarithmic diffusion in Ref. [38].

The theoretical predictions and the computer simulation results for the first two moments for selected values of α and λ are shown in Fig. 3. It is seen that the analytic results from

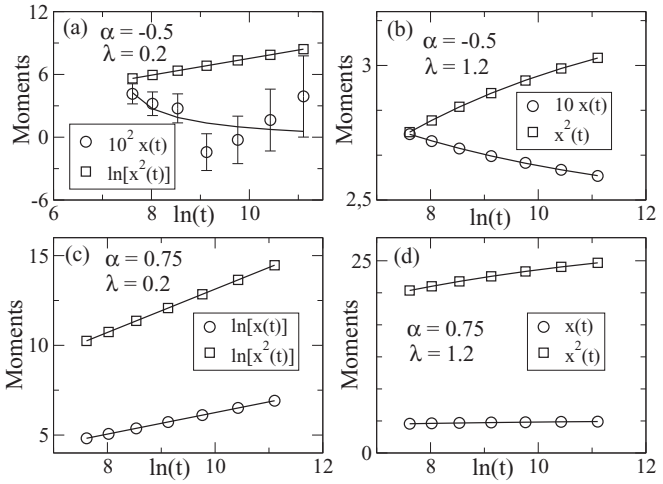

FIG. 3. Comparison between the theoretical predictions for the first and second moments (from Table I) and computer simulations, versus the natural logarithm of time. Averages were achieved with 3×10^6 runs with 10^5 time units each. The circles and squares represent computer simulation results for the first and second moments, respectively. The error bars are about the same size as the symbols used to represent the moments, except for the first moments in Fig. 3(a). In the latter case the first moment values are too small, leading to large fluctuations and poor fittings.

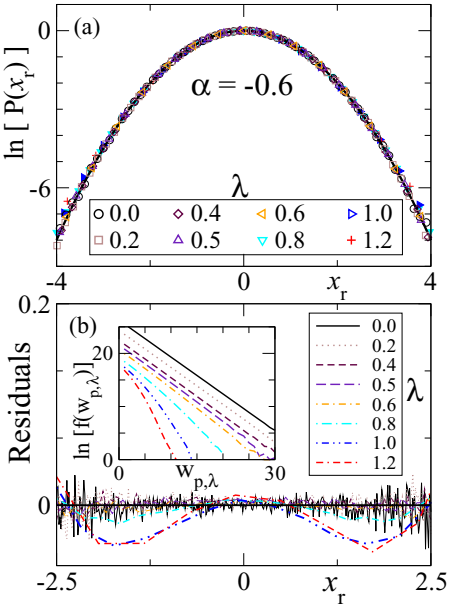

FIG. 4. (Color online) (a) The position PDFs for $\alpha = -0.6$ ($p = 0.2$) in a (natural)log-linear plot showing the frequency of occurrences of the position at $t_{max} = 10^6$ time units, against the normalized position ($x_r = [x - \langle x \rangle]/\sigma$). This provides a collapse of all data in a single Gaussian (solid line), represented by a parabola in this scale. (b) The residues of all data relative to the fitted parabola in the top panel showing the Gaussian deviations for $\lambda \geqslant 0.8$. The inset shows the PDFs of the persistence lengths $w_{p,\lambda}$ with the logarithm of the frequency in the vertical axis. The straight lines (exponential behavior) indicate that the position PDFs are Gaussian, pointing out to Gaussian statistics for $\lambda \leqslant 0.6$. Averages were accomplished with 50 000 runs and 10^6 time units each. These preliminary results shed some light on the transition from Gaussian to non-Gaussian behavior.

Table I are in accordance with the numerical simulations. It is interesting to note the large fluctuation values for the first moment in Fig. 3(a). This is due to the small values of $x(t)$ for $\lambda = 0.2$. In order to reduce the fluctuations and achieve better fittings, it would be necessary to increase cpu time by a factor of 100, at least.

Figure 4 shows the probability density functions of the position of the walker at t_{max} ($t_{max} = 50\,000$ and 10^7 numerical runs) for $\alpha = -0.6$ ($p = 0.2$). Figure 4(a) shows a Gaussian data collapse for several values of λ. The natural logarithm of the frequency is shown along the y axis against the position normalized as $[x - \langle x \rangle]/\sigma$ rendering Gaussians as parabolae. The solid line is a Gaussian fit to the $\lambda = 0$ numerical data, taken as a reference curve. We see an (apparent) overall good adjustment to the Gaussian curve. However, the residues shown in Fig. 4(b) indicate strong Gaussian deviations for $\lambda \geqslant 0.8$. The large residues are observed for $\lambda \geqslant 0.8$. These results are confirmed by the PDFs of the persistence length $w_{p,\lambda}$, defined as the time length of consecutive steps. They are shown in the inset, in a (natural)log-linear plot, with the logarithm of the number of occurrences in the y axis. A straight line in this plot represents an exponential distribution, which is known to be associated with a Gaussian statistics for the position distribution. We notice that this is the case up to $\lambda = 0.6$. For $\lambda \geqslant 0.8$, the persistence length data is inconclusive.

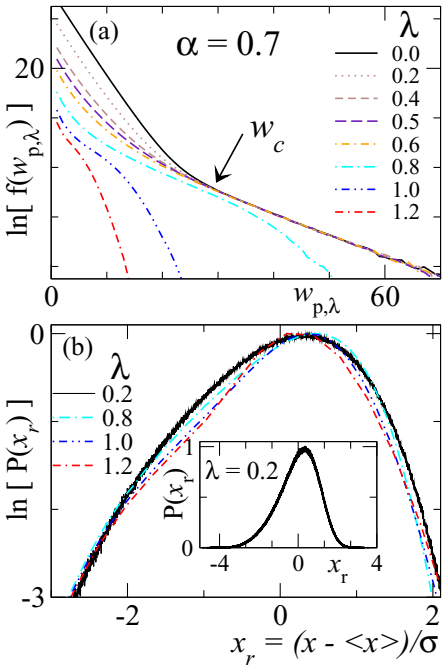

FIG. 5. (Color online) (a) The PDFs of the persistence lengths $w_{p,\lambda}$ for $\alpha = 0.7$ ($p = 0.85$) in a (natural)log-linear scale. Notice that there exists a pair of characteristic values (w_c,λ_c) such that the PDFs collapse for $w_{p,\lambda} \geqslant w_c$ and $\lambda \leqslant \lambda_c$ ($\lambda_c \lessapprox 0.8$ in the figure). In (b) the position distribution of the walker $P(x)$ is shown for selected values of λ against the normalized position $x_r = [x - \langle x\rangle]/\sigma$. The inset shows the shape of $P(x)$ in a linear-linear scale for $\lambda = 0.2$. Averages were obtained with 50 000 runs and 10^6 time units each. Notice the data collapse for $\lambda < 0.8$, which is surprising since it includes superdiffusive as well as subdiffusive regimes.

However, the statistics is non-Gaussian, as indicated by the residues. The important point to notice is that Gaussian and non-Gaussian statistics are supported within the subdiffusive regime in region (i) of Fig. 1. For $\alpha = -1$ ($p = 0$) the behavior of the PDFs with λ are similar to that for $\alpha = -0.6$ ($p = 0.2$), with smaller Gaussian deviations. The results are not shown here for reasons of space.

The persistence length is shown in Fig. 5(a), where we plot the natural logarithm of the frequency of occurrences of a given $w_{p,\lambda}$ for several values of λ and fixed $p = 0.85$, thereby crossing the superdiffusive regime and all the other phases of the model. The collapse of the PDFs for $\lambda < 0.8$ for large values of the persistence length is immediately noticeable. This result is very surprising, especially because it represents a collective behavior associated with two very different regions of the phase diagram, namely the superdiffusive and subdiffusive regions. The absence of exponential PDFs for $f(w_{p,\lambda})$ is compatible with the non-Gaussian PDFs for the position, shown in Fig. 5(b). Only some selected cases are shown for clarity. Notice that the logarithmic scale in the vertical axis of Fig. 5(b) would lead to a parabola for a Gaussian distribution. The inset shows the position PDF for $\lambda = 0.2$ in a linear-linear scale (frequency normalized to unity) displaying a negative skewness.

We emphasize that these are preliminary results, which need further investigations in order to establish the definitive character of these PDFs and, for example, the meaning of the collapse in Fig. 5, or the value of λ for which the Gaussian deviations begin in Fig. 4.

VIII. CONCLUSIONS

In summary, we have formulated a non-Markovian discrete-time random-walk model with pauses subjected to long-range time memory correlations. The equations of motion are derived and solved exactly for the first two moments. The Hurst exponents are obtained exactly and the rich phase diagram is fully characterized. The transitions from one diffusion type to another are also described in detail. Preliminary results for the position probability density functions at large times are shown along with the persistence lengths distributions. The Gaussian and non-Gaussian aspects of the model's statistics are discussed.

The model is expected to find suitable applications in processes where traps and subdiffusion play a role. These are, for example, in processes involving the first passage time density (FPTD) (see Ref. [12] for details and more references), in reaction-diffusion processes like $A + B \to B$, where B represents a transient (random) trapping condition, and hopefully in sociobiology, where diffusion is governed by subdiffusion or ultraslow diffusion. A continuous time generalization of the ERW model with traps would be notably important, and helpful for finding practical applications. This can possibly be done by following the same steps used in the continuous-time generalization of the ERW model carried out by Paraan and Esguerra [65].

It is worth emphasizing the similarities between these results and those obtained by Wang and Tokuyama [38], in which they analyze the influence of a frictional force upon a one-dimensional particle using the generalized Langevin equation. The phase diagram obtained by Wang and Tokuyama contains almost all diffusive regimes we put forward in this paper. Their continuous time GLE approach contrasts with our discrete-time random-walk method that explores directly the microscopic dynamics followed by the particle.

ACKNOWLEDGMENTS

J.C.C. and M.A.A.S. acknowledge FAPESP [Grants No. 2011/13685-6 (J.C.C.) and No. 2011/06757-0 (M.A.A.S.)] for financial assistance. G.M.V. thanks CNPq.

APPENDIX: CALCULATION OF THE SECOND MOMENT

1. Second moment for $\lambda \neq 1$

In order to determine $x_2(t)$ for $\lambda \neq 1$, we use Eqs. (15) and (16) for $\langle \sigma_{t+1} X_t\rangle = \langle \sigma^e_{t+1} X_t\rangle$. The expression for $\sigma^{\rm eff}_{t+1}$ comes from Eq. (6). We obtain

$$\left\langle X^2_{t+1}\right\rangle = \left\langle X^2_t\right\rangle + \frac{2\alpha A t^{-\lambda}}{A_0 + [A/(1-\lambda)]t^{1-\lambda}}\left\langle X^2_t\right\rangle + At^{-\lambda}.$$

Therefore, we can write an expression for the time derivative of the second moment, i.e.,

$$\frac{dx_2}{dt} = \frac{2\alpha A t^{-\lambda}}{A_0 + [A/(1-\lambda)]t^{1-\lambda}}x_2 + At^{-\lambda} \quad (\lambda \neq 1),$$

where $x_2(t) \equiv \langle x_2(t)\rangle$.

Integration gives

$$x_2(t) = \left(\frac{A}{1-\lambda}t^{1-\lambda} + A_0\right)^{2\alpha} \times \left[\int \frac{At^{-\lambda}}{\left(A_0 + \frac{A}{1-\lambda}t^{1-\lambda}\right)^{2\alpha}}dt + C_0\right], \quad \text{(A1)}$$

where C_0 can be determined with the initial condition $x_2(t = t_0) = x_0^2$.

For $\lambda < 1$ and $t \gg t_0$, we obtain, from Eq. (A1),

$$x_2(t) \sim \frac{A}{(1-\lambda)(1-2\alpha)}t^{1-\lambda} \quad (\lambda < 1, \alpha < 1/2),$$

$$x_2(t) \sim \frac{C_0 A^{2\alpha}}{(1-\lambda)^{2\alpha}}t^{2\alpha(1-\lambda)} \quad (\lambda < 1, \alpha > 1/2),$$

and

$$x_2(t) \sim At^{1-\lambda}\ln t \quad (\lambda < 1, \alpha = 1/2).$$

For $\lambda > 1$ and $t \gg 0$, we have, from Eq. (A1),

$$x_2(t) \sim \frac{A_0}{2\alpha}\ln[A_0(\lambda-1)] + C_0 A_0^{2\alpha} - \frac{A}{\lambda-1}\left(1 + \ln[A_0(\lambda-1)] + 2\alpha C_0 A_0^{2\alpha-1}\right)t^{1-\lambda}. \quad \text{(A2)}$$

2. Second moment for $\lambda = 1$

For $\lambda = 1$ we use Eqs. (15) and (16), along with Eq. (7) for $\sigma_{t+1}^{\text{eff}}$. We can write,

$$\langle X_{t+1}^2\rangle = \langle X_t^2\rangle + 2\frac{A\alpha(1-\lambda)}{t[t_0 + A\ln(t/t_0)]}\langle X_t^2\rangle + At^{-\lambda},$$

which gives a differential equation for $x_2(t)$, namely,

$$\frac{dx_2}{dt} = 2\frac{A\alpha(1-\lambda)}{t[t_0 + A\ln(t/t_0)]}x_2 + At^{-\lambda}. \quad \text{(A3)}$$

This equation must be integrated separately, according to the value of α. For $\alpha \neq 1/2$, the solution of Eq. (A3) is given by

$$x_2(t) = C_1[t_0 + A\ln(t/t_0)]^2 + \frac{t_0 + A\ln(t/t_0)}{1-2\alpha}.$$

For $t = t_0$ we use $x_0^2 = C_1 t_0^{2\alpha} + t_0/(1-2\alpha)$ to get $C_1 = (1/t_0^{2\alpha})[x_0^2 - t_0/(1-2\alpha)]$. For $\alpha = 1/2$, the solution of Eq. (A3) has a logarithmic correction to the power law, i.e.,

$$x_2(t) = [t_0 + A\ln(t/t_0)]\ln[t_0 + A\ln(t/t_0)] + C_2[t_0 + A\ln(t/t_0)].$$

For $t = t_0$ we have $\langle X_t^2\rangle = x_0^2$, which gives $x_0^2 = t_0\ln t_0 + C_2 t_0$ and $C_2 = x_0^2/t_0 - \ln t_0$.

[1] H. E. Hurst, R. P. Black, and Y. M. Simaika, *Long-Term Storage: An Experimental Study* (Constable, London, 1965).
[2] J. P. Bouchaud and A. Georges, Phys. Rep. **195**, 127 (1990).
[3] G. Weiss, *Aspects and Applications of the Random Walk* (North-Holland, Amsterdam, 1994).
[4] B. D. Hughes, *Random Walks and Random Environments*, Vol. 1: Random Walks (Oxford University Press, Oxford, 1995).
[5] R. Metzler and J. Klafter, Phys. Rep. **339**, 1 (2000).
[6] G. Radons, R. Klages, and I. M. Sokolov, *Anomalous Transport* (Wiley-VCH, Berlin, 2008).
[7] B. J. West and W. Deering, Phys. Rep. **246**, 1 (1994).
[8] L. F. Richardson, Proc. R. Soc. **110**, 709 (1926); cases with $H > 1$ are known, although very rare.
[9] R. N. Mantegna and H. E. Stanley, *An Introduction to Econophysics: Correlations and Complexity in Finance* (Cambridge University Press, Cambridge, 1999).
[10] A. Pękalski and K. Sznajd-Weron (eds.), *Anomalous Diffusion: From Basics to Applications* (Springer, Berlin, 1999).
[11] R. Metzler, E. Barkai, and J. Klafter, Phys. Rev. Lett. **82**, 3563 (1999).
[12] R. Metzler and J. Klafter, J. Phys. A: Math. Gen. **37**, R161 (2004).
[13] C. Nicolis and G. Nicolis, Phys. Rev. E **80**, 061119 (2009).
[14] R. J. Harris and H. Touchette, J. Phys. A **42**, 342001 (2009).
[15] E. K. Lenzi, H. V. Ribeiro, J. Martins, M. K. Lenzi, G. G. Lenzi, and S. Specchia, Chem. Eng. J. **172**, 2 (2011).
[16] W. D. Spencer, J. Mammal. **93**, 929 (2012).
[17] S. Havlin and D. Ben-Avraham, Adv. Phys. **36**, 695 (1987).
[18] M. Grifoni and P. Hänggi, Phys. Rep. **304**, 229 (1998).
[19] M. F. Shlesinger, G. M. Zaslavsky, and J. Klafter, Nature **363**, 31 (1993).
[20] M. F. Shlesinger, G. M. Zaslavsky, and U. Frisch (eds.), *Lévy Flights and Related Topics* (Springer, Berlin, 1995).
[21] J. Klafter, M. F. Shlesinger, and G. Zumofen, Phys. Today **49**, 33 (1996).
[22] R. Kutner, A. Pękalski, and K. Sznajd-Weron (eds.), *Anomalous Diffusion: From Basics to Applications* (Springer, Berlin, 1999).
[23] G. H. Weiss and R. J. Rubin, Adv. Chem. Phys. **52**, 363 (1983).
[24] S. Alexander, J. Bernasconi, W. R. Schneider, and R. Orbach, Rev. Mod. Phys. **53**, 175 (1981).
[25] M. B. Isichenko, Rev. Mod. Phys. **64**, 961 (1992).
[26] J. W. Haus and K. W. Kehr, Phys. Rep. **150**, 263 (1987).
[27] R. Balescu, *Statistical Dynamics, Matter out of Equilibrium* (Imperial College Press, London, 1997).
[28] A. Plonka, Ann. Rep. Prog. Chem. Sec. C **94**, 89 (1997).
[29] G. M. Zaslavsky and S. Benkadda, *Chaos, Kinetics and Nonlinear Dynamics in Fluids and Plasmas* (Springer, Berlin, 1998).
[30] R. Golestanian, Phys. Rev. Lett. **102**, 188305 (2009).
[31] P. Brault, C. Josserand, J.-M. Bauchire, A. Caillard, C. Charles, and R. W. Boswell, Phys. Rev. Lett. **102**, 045901 (2009).
[32] A. Mertelj, L. Cmok, and M. Copic, Phys. Rev. E **79**, 041402 (2009).
[33] C. D. Ball, N. D. MacWilliam, J. K. Percus, and R. K. Bowles, J. Chem. Phys. **130**, 054504 (2009).
[34] Y. Caspi, D. Zbaida, H. Cohen, and M. Elbaum, Macromolecules **42**, 760 (2009); R. Metzler, G. Glockle, and T. F. Nonnenmacher, Physica A **211**, 13 (1994); V. V. Saenko, Plasma Phys. Rep. **35**, 1 (2009).

[35] J.-H. Jeon, V. Tejedor, S. Burov, E. Barkai, C. Selhuber-Unkel, K. Berg-Sørensen, L. Oddershede, R. Metzler, Phys. Rev. Lett. **106**, 048103 (2011); N. Leijnse, J. H. Jeon, S. Loft, R. Metzler, and L. B. Oddershedel, Eur. Phys. J. Special Topics **204**, 75 (2012); S. C. Weber, A. J. Spakowitz, and J. A. Theriot, Phys. Rev. Lett. **104**, 238102 (2010).

[36] J. H. Jeon and R. Metzler, Phys. Rev. E **81**, 021103 (2010).

[37] I. Golding and E. C. Cox, Phys. Rev. Lett. **96**, 098102 (2006); R. J. Ellis and A. P. Minton, Nature **425**, 27 (2003); G. Seisenberger, M. U. Ried, T. Endre, H. Büning, M. Hallek, and C. Bräuchle, Science **294**, 1929 (2001).

[38] K. G. Wang and M. Tokuyama, Physica A **265**, 341 (1999).

[39] T. Geisel and S. Thomae, Phys. Rev. Lett. **52**, 1936 (1984).

[40] G. Zumofen and J. Klafter, Phys. Rev. E **47**, 851 (1993).

[41] R. Kubo, M. Toda, and N. Hashitsume, *Statistical Physics II Solid State Sciences*, Vol. 31 (Springer, Berlin, 1985).

[42] K. G. Wang, L. K. Dong, X. F. Wu, F. W. Zhu, and T. Ko, Physica A **203**, 53 (1994).

[43] J. M. Porra, K. G. Wang, and J. Masoliver, Phys. Rev. E **53**, 5872 (1996).

[44] E. Lutz, Phys. Rev. E **64**, 051106 (2001).

[45] V. Kobelev and E. Romanov, Prog. Theor. Phys. Suppl. **139**, 470 (2000).

[46] B. O'Shaughnessy and I. Procaccia, Phys. Rev. Lett. **54**, 455 (1985).

[47] E. W. Montroll and G. H. Weiss, J. Math. Phys. (NY) **6**, 167 (1965).

[48] H. Scher and E. W. Montroll, Phys. Rev. B **12**, 2455 (1975).

[49] M. F. Shlesinger, J. Stat. Phys. **10**, 421 (1974).

[50] H. Scher, M. F. Shlesinger, and J. T. Bendler, Phys. Today **44**, 26 (1991).

[51] D. Bedeaux, K. Lakatos-Lindenberg, and K. E. Shuler, J. Math. Phys. **12**, 2116 (1971); V. M. Kenkre, E. W. Montroll, and M. F. Shlesinger, J. Stat. Phys. **9**, 45 (1973); I. Oppenheim, K. E. Shuler, and G. H. Weiss (eds.), *Stochastic Processes in Chemical Physics: The Master Equation* (MIT Press, Cambridge, Massachusetts, 1977); V. M. Kenkre, Phys. Lett. A **65**, 391 (1978).

[52] C. Tsallis, S. V. F. Levy, A. M. C. Souza, and R. Maynard, Phys. Rev. Lett. **75**, 3589 (1995).

[53] V. Latora, A. Rapisarda, and C. Tsallis, Phys. Rev. E **64**, 056134 (2001).

[54] A. V. Chechkin, R. Gorenflo, and I. M. Sokolov, J. Phys. A: Math. Gen. **38**, L679 (2005).

[55] Edited by R. Hilfer, *Applications of Fractional Calculus in Physics* (World Scientific, Singapore, 2000).

[56] P. A. Santoro, J. L. de Paula, E. K. Lenzi, and L. R. Evangelista, J. Chem. Phys. **135**, 114704 (2011).

[57] Y. G. Sinai, Theor. Probl. Appl. **27**, 256 (1982).

[58] F. Igloi, L. Turban, and H. Rieger, Phys. Rev. E **59**, 1465 (1999).

[59] J. Dräger and J. Klafter, Phys. Rev. Lett. **84**, 5998 (2000).

[60] A. V. Chechkin, R. Gorenflo, and I. M. Sokolov, Phys. Rev. E **66**, 046129 (2002).

[61] A. V. Chechkin, J. Klafter, and I. M. Sokolov, Europhys. Lett. **63**, 326 (2003).

[62] D. Boyer, M. C. Crofoot, and P. D. Walsh, J. R. Soc. Interface **9**, 842 (2012).

[63] L. Bachelier, Ann. Sci. Ec. Normale Super. **17**, 21 (1900); A. Einstein, Ann. Phys. (Leipzig) **17**, 549 (1905); S. Chandrasekhar, Rev. Mod. Phys. **15**, 1 (1943); B. B. Mandelbrot, *Multifractals and 1/f Noise: Wild Self-Affinity in Physics* (Springer, New York, 1999).

[64] G. M. Schütz and S. Trimper, Phys. Rev. E **70**, 045101 (2004).

[65] F. N. C. Paraan and J. P. Esguerra, Phys. Rev. E **74**, 032101 (2006).

[66] J. C. Cressoni, Marco Antonio Alves da Silva, and G. M. Viswanathan, Phys. Rev. Lett. **98**, 070603 (2007).

[67] N. Kumar, U. Harbola, and K. Lindenberg, Phys. Rev. E **82**, 021101 (2010).

[68] M. Kac, Am. Math. Mon. **54**, 369 (1947).

[69] M. R. King, Fractals **12**, 235 (2004).

[70] T. Kuusela, Phys. Rev. E **69**, 031916 (2004).

[71] L. Klimeš, Pure Appl. Geophys. **159**, 1811 (2002).

[72] J. Schmittbuhl, G. Chambon, A. Hansen, and M. Bouchon, Geophys. Res. Lett. **33**, L13307 (2006).

[73] M. Tarafder, I. Chattoraj, S. Tarafder, and M. Nasipuri, Mater. Sci. Technol. **25**, 542 (2009).

[74] J. Kalda, Europhys. Lett. **84**, 46003 (2008).

[75] Marco Antonio Alves da Silva, G. M. Viswanathan, A. S. Ferreira, and J. C. Cressoni, Phys. Rev. E **77**, 040101 (2008).

[76] M. A. A. da Silva, J. C. Cressoni, G. M. Schütz, G. M. Viswanathan, and S. Trimper, Phys. Rev. E **88**, 022115 (2013).

[77] B. D. Malamud and D. L. Turcotte, J. Stat. Plan. Inf. **80**, 173 (1999).

[78] F. Serinaldi, Physica A **389**, 2770 (2010).